

Hydroxymethyl PEDOT microstructure-based electrodes for high-performance supercapacitors

Cite as: APL Mater. 10, 061101 (2022); <https://doi.org/10.1063/5.0088452>

Submitted: 17 February 2022 • Accepted: 10 May 2022 • Published Online: 03 June 2022

 Shofarul Wustoni, Georgios Nikiforidis,  Sahika Inal, et al.



View Online



Export Citation



CrossMark

ARTICLES YOU MAY BE INTERESTED IN

[MXene improves the stability and electrochemical performance of electropolymerized PEDOT films](#)

APL Materials 8, 121105 (2020); <https://doi.org/10.1063/5.0023187>

[Extinction coefficient measurement of supercritical water-based multi-walled carbon nanotube nanofluids](#)

AIP Advances 12, 065305 (2022); <https://doi.org/10.1063/5.0086358>

[Perception of interrupted speech and text: Listener and modality factors](#)

JASA Express Letters 2, 064402 (2022); <https://doi.org/10.1121/10.0011571>

APL Materials

Special Topic: Design and
Development of High Entropy Materials

Submit Today!



Hydroxymethyl PEDOT microstructure-based electrodes for high-performance supercapacitors

Cite as: APL Mater. 10, 061101 (2022); doi: 10.1063/5.0088452

Submitted: 17 February 2022 • Accepted: 10 May 2022 •

Published Online: 3 June 2022



View Online



Export Citation



CrossMark

Shofarul Wustoni,^{1,2,a)}  Georgios Nikiforidis,³ Sahika Inal,⁴  Yuli Setyo Indartono,² Veinardi Suendo,¹ 
and Brian Yulianto^{2,a)}

AFFILIATIONS

¹Department of Chemistry, Institut Teknologi Bandung, Bandung 40132, Indonesia

²Research Center for New and Renewable Energy, Institut Teknologi Bandung, Bandung 40132, Indonesia

³UCL Institute for Materials Discovery, University College London, Malet Place, London WC1E 7JE, United Kingdom

⁴Biological and Environmental Science and Engineering, King Abdullah University of Science and Technology, Thuwal 23955-6900, Saudi Arabia

Note: This paper is part of the Special Topic on Materials Challenges for Supercapacitors.

a) Authors to whom correspondence should be addressed: s.wustoni@itb.ac.id and brian@tf.itb.ac.id

ABSTRACT

The development of conducting polymer-based supercapacitors offers remarkable advantages, such as good ionic and electronic conductivity, ease of synthesis, low processing cost, and mechanical flexibility. 3,4-ethylenedioxythiophene (PEDOT) is a conducting polymer with robust chemical and environmental stability during storage and operation in an aqueous environment. Yet, improving its electrochemical capacitance and cycle life remains a challenge for high-performance supercapacitors exceeding the current state-of-the-art. The fabrication of PEDOT composites with carbon nanomaterials and metal oxides is the commonly used approach to enhance capacitance and stability. This work discusses a comparative study to fabricate highly stable PEDOT derivative electrodes with remarkable specific capacitance via a straight-forward electrochemical polymerization technique. The hydroxymethyl PEDOT (PEDOTOH) doped with perchlorate in a dichloromethane (DCM) solvent (197 F g^{-1}) exhibits superior performance compared to the polymer formed in an aqueous solution (124 F g^{-1}). Furthermore, the electropolymerized PEDOTOH on flexible Au/Kapton substrates was assembled into a free-standing symmetrical supercapacitor in an agarose additive-free gel. The use of agarose gel electrolytes can offer easy handling, no leakage, moderate ionic conductivity, and flexibility for miniaturization and integration. The supercapacitor reached a specific capacitance of 36.96 F g^{-1} at a current density of 13.7 A g^{-1} , an energy density of 14.96 Wh kg^{-1} , and a power density of 22.2 kW kg^{-1} among the highest values reported for PEDOT-based supercapacitors. The self-standing supercapacitor achieves an industry-par capacitance retention of $\sim 98\%$ after 10000 charge/discharge cycles at 10 A g^{-1} . This study provides insights into the effect of solvents and electropolymerization modes on the polymer structure and its electrochemical properties toward high-performance supercapacitor devices.

© 2022 Author(s). All article content, except where otherwise noted, is licensed under a Creative Commons Attribution (CC BY) license (<http://creativecommons.org/licenses/by/4.0/>). <https://doi.org/10.1063/5.0088452>

INTRODUCTION

Energy storage devices have become emerging tools to stockpile sustainable energy sources and thrift energy transmission efficiency. With that in mind, supercapacitors have received tremendous interest as energy storage devices since they can provide high power density ($>100 \text{ Wh/kg}$), fast charging/discharging (seconds to milliseconds), and superior cycleability ($>500\,000$ cycles) than batteries.¹ Due to these features, supercapacitors can

fulfill the demand in a variety of applications, including handling the power fluctuations in the grid, storing the energy from regenerative braking, and powering hybrid electric vehicles.² The material selection of supercapacitor electrodes depends on the device design and the working mechanism. The primary categories of supercapacitors based on the charge storage mechanism encompass electrical double-layer capacitors (EDLC), pseudocapacitors, and hybrid supercapacitors.^{3,4} Carbon-based materials, such as activated carbon, carbon aerogel, graphene, and carbon nanotubes,

are typical EDLC electrodes, absorbing ions on their surface and forming double-layer capacitances. For instance, activated carbon with a surface area of $1000 \text{ m}^2 \text{ g}^{-1}$ can produce a double-layer capacitance of $10 \text{ } \mu\text{F cm}^{-2}$. Pseudocapacitors comprise electrodes such as conducting polymers and metal oxides that can undergo reversible redox reactions and store the charges both on the surface and/or the bulk through electrosorption or intercalation.^{5,6} They can generate higher energy and power density compared to EDLC; however, they suffer from structural stability during repetitive redox cycling.⁷ To this end, there is room for improvement in pseudocapacitive materials aspiring to achieve high performance and stability.

Conducting polymers are one of the most exciting groups of pseudocapacitive materials due to their high electrical conductivity, reversible redox states, ease of synthesis, and mechanical flexibility.^{8,9} There is a wide variety of conducting polymers that have been extensively explored for supercapacitor applications, including polyaniline (PANI), polypyrrole (PPy), and poly(3,4-ethylenedioxythiophene) (PEDOT).¹⁰ Among these, PEDOT offers better chemical stability, environmental stability, biocompatibility, a wider potential window, and broader operating temperature (i.e., thermal stability).¹¹ The PEDOT-based electrodes have been widely explored in numerous applications, including bioelectronics, thermoelectric, and particularly energy storage devices (e.g., supercapacitors and batteries).^{11–14} However, pristine PEDOT electrodes are unstable upon repetitive cycling, and their capacitance is lower compared to other pseudocapacitive materials.¹⁰ Various strategies have been explored in the past decade, mainly on the synthesis of PEDOT composites with carbon nanomaterials and metal oxides. For instance, Tang *et al.*¹⁵ developed hybrid graphite/PEDOT/MnO₂ electrodes and achieved a specific capacitance of 195.7 F g^{-1} . Ahmed and Rafat¹⁶ and He *et al.*¹⁷ reported the fabrication of PEDOT composites with reduced graphene oxide (rGO) and carbon nanotubes (CNTs), respectively, boosting the capacitance and stability of their PEDOT-based electrodes. Yet, the majority of processes of PEDOT nanocomposite fabrication involve multiple steps, the use of hazardous reagents and additives, and post-processing treatments, leading to long fabrication time and high production cost. In this vein, straightforward and simple techniques for developing native PEDOT electrodes with improved capacitance and stability are desirable for routine and long-term supercapacitor operation.

In recent years, various strategies have been proposed to develop simple polymerization techniques that can generate PEDOT with different structures, doping levels, and counterions. Material structure and surface morphology can substantially tune the electrochemical properties to achieve more extensive storage capability, a kinetically faster charge storage process, and cycling stability.¹⁸ Researchers have created different recipes to construct novel PEDOT electrodes with nano- and microstructures through various polymerization techniques, including oxidative chemical polymerization, vapor phase polymerization, and electrochemical polymerization. In the case of chemical oxidative method in the solution phase, despite the high polymerization yield, this method lacks control from the batch-to-batch mode due to the impurity of excess oxidizers, counterions, and catalysts while also the low solubility during the purification process. On the other hand, vapor phase polymerization has been widely used to obtain derivative

PEDOT-based supercapacitors with good intrinsic conductivity and minor impurity as opposed to the chemical polymerization method. Several works have demonstrated the use of vapor phase polymerization to prepare polycrystalline PEDOT nanostructures in the absence of hard templates (e.g., anodized aluminum oxide). D'Arcy *et al.* produced high aspect ratio PEDOT nanofibers deposited from vapor phase methods.¹⁹ Such a PEDOT nanofibrillar electrode has shown a specific capacitance of 175 F g^{-1} and a retention of 94% after 1000 cycles. Other works have examined the capability of vapor phase polymerization to induce morphological changes,²⁰ levels of crystallinity,²¹ and the doping level²² of PEDOT on different substrates, i.e., flexible paper. Yet, vapor phase polymerization requires high temperatures, which can be costly and time-consuming and constraint the polymer coating and coverage, resulting in a non-uniform PEDOT layer on the substrate.

To address the challenges, electrochemical polymerization poses as an alternative and promising method to accomplish a simple, robust, and cost-effective polymerization while enabling the tuning of different parameters for the practical improvement of PEDOT electrodes for supercapacitors. Electropolymerization can precisely deposit the PEDOT film in a specific geometrically electrode pattern with convenient control over the thickness and morphology through the process parameters, such as applied deposition methods, solvents, and counterions.^{23,24} Additionally, this method can also create a strong adhesion between the PEDOT film and the substrate.^{25,26} Although many electropolymerized PEDOT electrodes have been utilized in supercapacitors,^{27–29} their specific capacitance and cycling stability remain a major issue, and to the best of our knowledge, there is limited evidence on the native PEDOT electrode being able to achieve specific capacitance retention of 80%–90% over thousands of charge–discharge cycles unless combined with other nanomaterials and nanocomposites, which require extra materials and processing.

This study presents a robust symmetrical pristine PEDOT-based supercapacitor with excellent electrochemical stability. We demonstrate a straightforward electrochemical polymerization route to generate hydroxymethyl PEDOT, namely, PEDOTOH, on a flexible Au/Kapton substrate for supercapacitor application. The PEDOTOH electrodes produced in dichloromethane (DCM), a non-flammable solvent, exhibit a high specific capacitance (197 F g^{-1}) over the analog polymer film synthesized in an aqueous solution (i.e., 124 F g^{-1}). The specific capacitance is among the highest values reported for PEDOT-based electrodes in the literature. The PEDOTOH film revealed a uniform coating with microtube and microporous structures that are formed within 5 min with high active mass loading of 104 and $256 \text{ } \mu\text{g}$ in deionized (DI) water and DCM, respectively. The PEDOTOH electrodes are easily assembled in a symmetric supercapacitor engulfed by an agarose gel containing 1 M LiClO_4 as an electrolyte. The supercapacitor devices display high specific capacitances (73.7 F g^{-1} at a scan rate of 10 mV s^{-1}), excellent cycling stability (98% retention after 10000 GCD cycles at 10 A g^{-1}), and energy and power densities of 14.96 Wh kg^{-1} and 22.2 W kg^{-1} , respectively. These supercapacitors incorporated with gel electrolytes offer free-standing configuration, high specific capacitance, and excellent stability with simple, non-flammable reagents and a fast polymerization method.

MATERIALS AND METHODS

Materials

3,4-ethylenedioxythiophene (EDOT), hydroxymethyl EDOT (EDOTOH), lithium perchlorate (LiClO_4), tetrabutylammonium perchlorate (TBAP), dichloromethane (DCM), and agarose low gelling temperature were purchased from Sigma-Aldrich and used as received. The aqueous solutions were prepared by using ultrapure water (Millipore Milli-Q).

Electrochemical polymerization of PEDOT and PEDOTOH electrodes

Flexible Kapton (polyimide) substrates ($175 \mu\text{m}$) are sputtered with 10 nm of Cr and 100 nm of Au layers and cut into a square geometry ($8 \times 8 \text{ mm}^2$) by a digital craft cutter (Silhouette). Prior to electropolymerization, the substrates were washed in isopropyl alcohol (IPA) and deionized (DI) water under sonication at room temperature. Subsequently, the substrates were electrochemically cleaned in 10 mM H_2SO_4 using cyclic voltammetry (CV) in the potential range of $-0.2 - 1.2 \text{ V}$ vs Ag/AgCl for twenty cycles (Corrtest Cs350). The electrochemical polymerizations were carried out in either the DCM solvent or aqueous solution. In the case of DCM, 10 mM of EDOT or EDOTOH was mixed with 100 mM TBAP, whereas 10 mM of EDOTOH was added with 100 mM LiClO_4 in an aqueous solution for comparative purposes. Electropolymerization was performed by using either potentiostatic mode at 1 V for 300 s or galvanostatic mode at 8 mA for 300 s. The electrodeposited polymer films were rinsed with DI water and sprayed with N_2 gas to remove excess monomers and weekly adsorbed materials on the surface. The mass (μg) of the polymer films was determined as the weight difference between bare Au/Kapton substrate before and after electropolymerization using a microbalance (Mettler Toledo).

Configuration of symmetrical PEDOTOH-based supercapacitors

The PEDOTOH electrodes were assembled into symmetrical supercapacitors facing each other at a distance of 2 mm within an agarose gel electrolyte as demonstrated in the previous study.³⁰ To prepare the agarose gel, 600 mg of agarose was dissolved in 10 ml of 1 M LiClO_4 to obtain 6 wt.% agarose content. The pre-gel solution was vigorously stirred on a hot plate at 90°C ; then, the solution was cast onto the template with the PEDOTOH electrodes at the above-mentioned distance. The gel was left to cure for 10 min at room temperature. This gel electrolyte prevents the shorting of the electrodes and assures the electrical connectivity between the cathode and the anode without a separator. The embedded electrodes inside the agarose gel containing ions form self-standing all-polymer supercapacitors, as illustrated in Fig. 1(d). During the electrochemical measurement of the supercapacitor, the device was wetted every 3 h with $100 \mu\text{l}$ of 1 M LiClO_4 .

Electrochemical evaluation of the PEDOTOH-based electrodes and assembled supercapacitors

Electrochemical measurements of deposited polymer electrodes as working electrodes were performed using the three-electrode configuration in 1 M LiClO_4 at room temperature. Ag/AgCl and Pt wire were used as reference electrode and counter electrode, respectively. The electrochemical properties, such as specific capacitance and cycling stability, were evaluated by cyclic voltammetry (CV) and galvanostatic charge-discharge (CGD) using potentiostat Corrtest CS350. The specific capacitance of the electrodes and the assembled supercapacitors was calculated from either CV at a particular scan rate or GCD at a set current density. The specific capacitance ($C_s, \text{F g}^{-1}$), which is the capacitance of one electrode per unit mass, was calculated using the

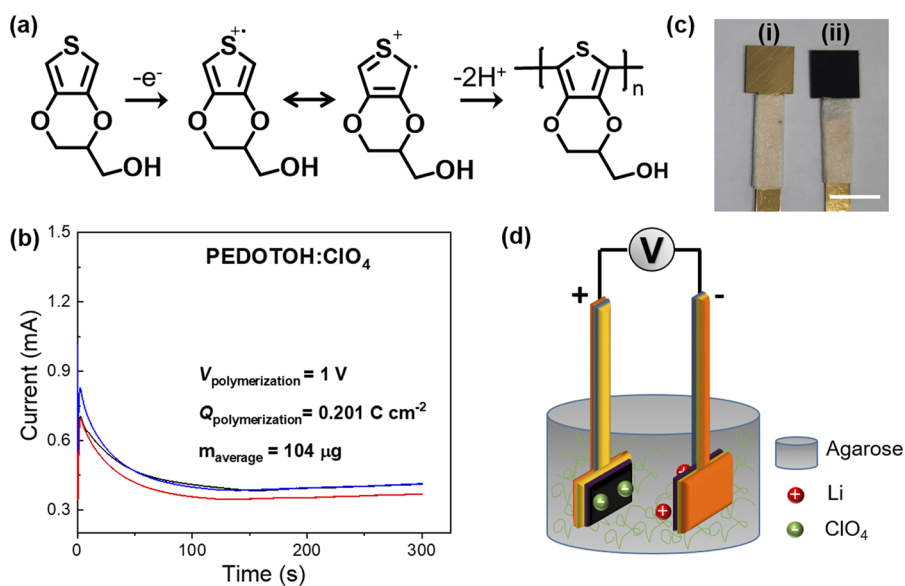


FIG. 1. Electrochemical polymerization of the PEDOTOH electrode and assembly of the supercapacitor. (a) The chemical structure and polymerization route of PEDOTOH, the polymer is drawn in its neutral state, and the ClO_4^- dopant is not shown. (b) Photograph of (i) bare Au coated polyimide (Kapton) substrates and (ii) deposited PEDOTOH films after electropolymerization. Scale bar is 8 mm. (c) Chronoamperometric curves recorded during the polymerization of PEDOTOH: ClO_4 in water under a constant potential of 1 V for 5 min. Triplicate experiments were conducted for each sample. (d) A schematic illustration of the assembled PEDOTOH electrodes as the cathode and anode in an agarose gel-based electrolyte for the supercapacitor.

following equations from CV curves [Eq. (1)] and GCD plots [Eq. (2)]:

$$C_s = \frac{Q}{2\mu m \Delta V}, \quad (1)$$

$$C_s = \frac{i \Delta t}{\Delta V}, \quad (2)$$

where Q is the total charge in coulombs by calculating the integral area of the CV curve and μ and ΔV represent the scan rate and the potential window of the CV cycle, respectively. While m is the mass of each electrode. For Eq. (2), i is the discharge current density ($A\ g^{-1}$) and Δt and ΔV are the discharge time and potential window, respectively. In addition, the capacitance retention of the electrode and supercapacitors was evaluated by using CV and GCD for multiple cycles within a potential window lying between -0.2 and 0.7 V. The energy (E , Wh kg^{-1}) and power density (P , W kg^{-1}) were extracted from the GCD curves from the following equations:

$$E = \frac{C_s (\Delta V)^2}{2}, \quad (3)$$

$$P = \frac{E \times 3600}{\Delta t}. \quad (4)$$

The Coulombic efficiency ($n_{\text{coulombic}}$) of the supercapacitors was evaluated as the ratio between the discharging and charging times within -0.2 and 0.7 V as displayed in the following:

$$n_{\text{coulombic}} = \frac{\text{Total charge released}}{\text{Total charge stored}} = \frac{\text{Discharging time}}{\text{Charging time}}. \quad (5)$$

Electrochemical impedance spectroscopy (EIS) of the electrodes and supercapacitor devices was examined at 0 V vs the open-circuit potential. The AC amplitude was 10 mV, while the frequencies varied between 0.1 Hz and 100 kHz.

Physicochemical characterization of the PEDOTOH-based electrodes

The chemical composition of the electrode film after electropolymerization was evaluated by using Fourier transform infrared (FTIR). The FTIR spectra were recorded in the range 550 – 4000 cm^{-1} at room temperature using Thermo Scientific Nicolet iS10. Attenuated total reflection (ATR) FTIR mode was used to obtain the reflectance infrared spectra of the polymer film. We signal-averaged 32 scans to form a single spectrum, then displayed in terms of transmittance. The baseline was corrected using OMNIC FTIR software. The surface morphology of the electrodeposited polymer film was characterized using an FEI Nova NanoSEM (scanning electron microscope) with an accelerating voltage of 3 kV and a working distance of 5 mm. The films were mounted onto aluminum stubs and attached with conductive tape.

RESULTS AND DISCUSSION

Electrochemical polymerization of PEDOTOH-based electrodes

We design a single-step electrochemical polymerization of conducting polymer electrodes using hydroxymethyl EDOT (EDO-TOH) monomer and ClO_4^- as the dopant. We chose the EDOTOH monomers as the building block of the polymer network since the previous studies have reported that such monomers could improve the electropolymerization efficiency and the resulting polymers exhibit higher electrochemical capacitance than native PEDOT.^{31–33} We selected a small dopant (viz., ClO_4^- , $r \sim 0.22$ nm³⁴) instead of polymeric dopant PSS^- due to its ability to produce rougher polymer films with a porous morphology that could increase the electrochemically active surface area, improving the capacitance of the polymer films. Figure 1(a) displays the electropolymerization routes when using the EDOTOH monomer under ambient conditions. The polymerization reaction starts with the oxidation of EDOTOH by an applied voltage of 1 V that leads to the formation of EDOTOH radical cations. These active species form dimers and extend into chain-growth polymerization. A five-min-long electropolymerization in DI water at 1 V yields PEDOTOH: ClO_4^- films with an average mass of 104 μg , while the charge consumed (Q_{pol}) during polymerization reaches 0.201 C cm^{-2} [Fig. 1(b)]. The chronoamperometric curve is identical with the typical electropolymerization curve of PEDOT from other studies, showing a sharp increase in the current at the beginning, attributed to the monomer oxidation and the nucleation stage, followed by a stabilized current signifying the polymer growth. The electrodeposited polymer films could also be evaluated by naked eye from their appearance on the flexible Au/Kapton substrate [Fig. 1(c)]. The electrodes were then assembled as the cathode and anode into a free-standing supercapacitor cell using agarose gel as an electrolyte [Fig. 1(d)].

We begin by performing a comparative analysis to enhance further the electrochemical properties of PEDOTOH-based electrodes, which have been studied in the context of electrochromic and actuator devices but are limited to energy storage applications.^{31,32,35,36} We examined the electrochemical synthesis of PEDOTOH: ClO_4^- polymerized in two different solvents, DI water and dichloromethane (DCM) (see the subsection Electrochemical polymerization of PEDOT and PEDOTOH electrodes in Materials and Methods for the electrochemical polymerization protocols). Although DI water entails a green chemistry approach, the electrodeposited polymer films suffer from feeble adhesion and require a template to form a porous structure. On the contrary, DCM is an alternative solvent that has shown the capability to generate a porous network of PEDOT film and has been recently used in bioelectronics devices for sensing.^{37,38} Thus, we investigate the effect of these two solvents on the fabricated PEDOTOH electrodes and their application in symmetrical two-electrode supercapacitors.

First, the electrochemical performances of PEDOTOH electrodes were examined by a three-electrode configuration in 1 M $LiClO_4$. Figure 2(a) shows the cyclic voltammogram of PEDOTOH electrodes at a scan rate of 10 mV s^{-1} , where typical rectangular curves are evident and indicate an ideal capacitor profile. From the CV curves, the PEDOTOH electrode fabricated in DCM delivers a specific capacitance of 197.3 F g^{-1} , markedly larger than the one of the PEDOTOH electrode formed in DI water (i.e., 124.9 F g^{-1}),

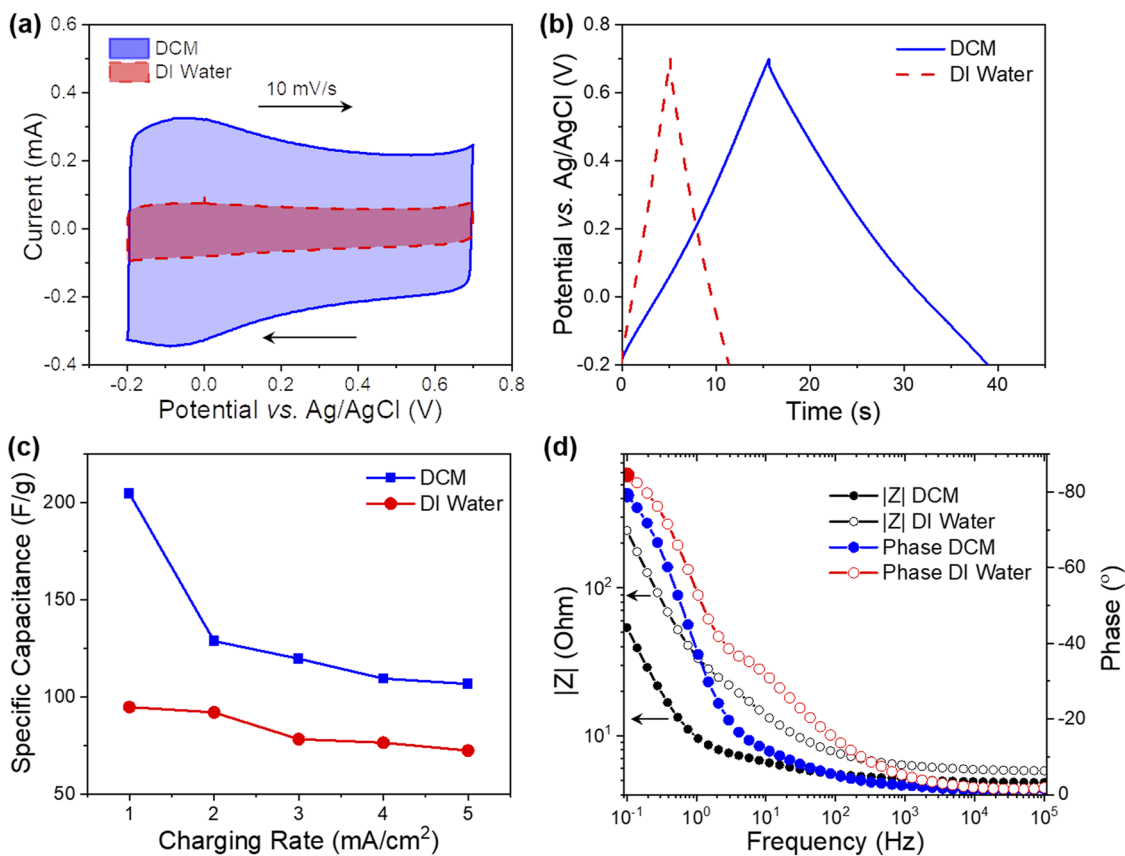


FIG. 2. The electrochemical analysis of the PEDOTOH films fabricated in DCM and aqueous solution. (a) CV curves at a scan rate of 10 mV s^{-1} over a potential window of -0.2 to 0.7 V vs Ag/AgCl. (b) Charge–discharge curves at 2 mA cm^{-2} . (c) Specific capacitance at different charging rates up to 5 mA cm^{-2} . (d) Magnitude and phase of the impedance of the PEDOTOH films performed at 0 V vs the open-circuit potential (V_{OC}). All electrochemical measurements were carried out in 1 M LiClO_4 at room temperature.

showing that the DCM solvent boosts the capacitive behavior of the deposited polymer with identical composition and electrode area ($8 \times 8 \text{ mm}^2$). Moreover, the CV curves of the PEDOTOH electrodes over a range of scan rates are given in Figs. S1(a) and S1(b). They preserve the rectangular shape at scan rates as high as 200 mV s^{-1} . By plotting the $\log(\text{current density})$ vs $\log(\text{scan rate})$, we analyzed further the charge storage mechanism according to the following formula:

$$i = av^b, \quad (6)$$

where i is the current density (A g^{-1}) taken at a specific potential in the different scan rates v while a and b are adjustable parameters. The b -value delineates the charge storage mechanism, where the value close to 0.5 indicates a diffusion-limited process and a b -value of 1 advocates a capacitive-controlled process. As shown in Figs. S1(c) and S1(d), by fitting the $\log(i)$ vs $\log(v)$, the b -values of PEDOTOH electrodes are 0.99 and 0.94 for the electrodes produced in DCM and DI water, respectively. The electrodes made in DCM exhibit a slightly higher b -value, indicative of a more kinetically capacitive charge storage substrate.

Figure 2(b) shows the galvanostatic charge–discharge (GCD) profiles of the PEDOTOH electrodes at a current density of 2 mA cm^{-2} (normalized by the geometrical surface area of the electrode, 0.64 cm^2). Both electrodes present ideal triangular shapes at any given current densities (Fig. S2), consistent with the rectangular CV profiles. The specific capacitance of the PEDOTOH electrodes at different current densities is plotted in Fig. 2(c). The CV and GCD measurements reveal that the PEDOTOH electrode fabricated in DCM reaches a specific capacitance of 204.7 F g^{-1} at a charging rate of 1 mA cm^{-2} (analogous to 2.5 A g^{-1}) or 197.3 F g^{-1} at a scan rate of 10 mV s^{-1} . This value is among the highest reported capacitance values for pristine PEDOT-based electrodes, such as vapor phase polymerized PEDOT (179 F g^{-1}),³⁹ PEDOT nanofibers (175 F g^{-1}),¹⁹ and also better than several PEDOT nanocomposites, including PEDOT/rGO (102.8 F g^{-1})¹⁶ and PEDOT:PSS/SWCNT (114 F g^{-1})⁴⁰ (Table S2). The above-mentioned specific capacitance of our fabricated electrode constitutes 97.5% of the theoretical capacity of PEDOT (210 F g^{-1}), validating the optimal chemical and physical properties of the fabricated PEDOTOH in the electrochemical charge storage mechanism. The PEDOTOH electrode properties

were further evaluated by using electrochemical impedance spectroscopy (EIS). The Bode plot provides insight into the electrodes' capacitive behavior and rate capability [Fig. 2(d)]. The impedance of PEDOTOH formed in DCM was lower than the one produced in DI water at all frequencies. For example, at a frequency of 0.1 Hz, the impedance of the PEDOTOH formed in DCM is $\sim 53.8 \Omega$ as opposed to 243.8Ω for the PEDOTOH formed in DI water. The phase angle of both electrodes approaches $\sim 80^\circ$ at low frequencies, connoting an ideal capacitive behavior (90°). The fitting of the Nyquist plots further confirmed that PEDOTOH formed in DCM has lower charge transfer resistance (R_{ct}) and higher double-layer capacitance than PEDOTOH formed in DI water (Fig. S3, Table S1). In addition, we extract the dielectric relaxation time constant (τ_0), which represents the minimum charge/discharge time to achieve 50% efficiency of the electrode performance from the frequency value at a phase angle of -45° (f_0). The f_0 values were ~ 0.75 and 1.8 Hz corresponding to τ_0 of 1.3 and 0.6 s for the electrodes fabricated in DCM and DI water, respectively. These τ_0 values outperform the time constant for several other polymer-based supercapacitor electrodes, representing fast and facile kinetic diffusion of ions in the polymer networks of our PEDOTOH electrode.

To benchmark the PEDOTOH performance against conventional PEDOT without hydroxymethyl side chains on the ethylenedioxy ring, we electrochemically synthesize a native PEDOT electrode in DCM under identical polymerization conditions. As shown in Fig. S4, the PEDOT:ClO₄ electrodes made in DCM reach a specific capacitance of 159.1 F g^{-1} at a charging rate of 1 mA cm^{-2} (2.3 A g^{-1}) and display ideal capacitive behavior from the CV and GCD plots, while the b -value is close to 1. The C_s value of PEDOT:ClO₄ in DCM is higher than that of PEDOTOH:ClO₄ in water, however, still lower than that of PEDOTOH:ClO₄ in DCM. Therefore, the electropolymerization in DCM enhances the electrochemical properties of the deposited polymer, while hydroxymethyl EDOT creates a more dense capacitive polymer network than the pristine EDOT.

Furthermore, we introduced another variation to fabricate PEDOTOH:ClO₄ in DCM by tuning the electropolymerization mode using galvanostatic (constant current) mode instead of potentiostatic (constant potential) mode since it is well-known that different electropolymerization modes produce different polymer structures. Figure S5 presents the CV and GCD profiles of PEDOTOH electrodes generated by galvanostatic mode in DCM. CV and GCD curves remain rectangular and triangular shapes at different scan rates and current densities with excellent rate capability. The calculated specific capacitance of this electrode is 148 F g^{-1} at a scan rate of 10 mV s^{-1} , which is lower than the polymer electrode formed using potentiostatic mode. This result indicates that different electropolymerization modes can yield a variation in

the PEDOTOH properties, including morphology, which induces their electrochemical capacitance capability. Table I displays a list of specific capacitances of each electrode fabricated in this work.

Physicochemical characterization of PEDOTOH films

To elucidate the difference in the polymer films fabricated in DCM and DI water, we first evaluate the chemical composition and the formation of PEDOTOH polymer chains using Fourier transform infrared (FTIR) spectroscopy.⁴¹ Figure 3(a) shows identical spectra of both PEDOTOH:ClO₄ fabricated in DCM and DI water with similar peak shapes and a negligible difference in relative intensity of the peaks, indicating that both polymers possess the same chemical bond environment. The FTIR spectra also revealed several characteristic bonds of PEDOT; for instance, the unique band of stretching vibration of the C–S–C bond in the thiophene chain can be observed at 637 , 807 , and 948 cm^{-1} . The vibration bands at 1271 and 1488 cm^{-1} are attributed to the stretching mode of C=C and inter-ring stretching mode of C–C in the thiophene chain.^{41,42} These bands confirmed the successful polymer formation of our PEDOTOH using electropolymerization both in DCM and DI water.

In addition, the topography of the PEDOTOH films was characterized by using scanning electron microscopy (SEM). The top-view SEM images [Figs. 3(b)–3(e)] revealed a distinct morphology of PEDOTOH:ClO₄ fabricated in DCM with the potentiostatic mode compared to other polymer films. The PEDOTOH sample revealed a rough surface containing a typical tube-like structure with open ends. In contrast, the other polymer films were relatively uniform with a few agglomerates on their surface. This unique microtube structure, interestingly, can be only obtained by combining EDOH monomers in a DCM medium with potentiostatic mode. Such a porous network of microtubes brings several advantages, including (i) an interconnected network that can facilitate ion transport pathways and (ii) enlargement of the electrochemically active surface area. The increased surface area and ions pathway can significantly improve the reactive sites in the polymers' electrochemical doping/dedoping reaction, thus leading to a superior electrochemical capacitance.

Electrochemical stability of PEDOTOH films

Next, we examine the electrochemical stability of the PEDOTOH electrodes, which is an essential property for any electronic films operated at the interface with electrolytes. In general, most of the polymer-based electrodes experience mechanical stress during ion intercalation/deintercalation on the bulk polymer networks,

TABLE I. Specific capacitances of PEDOTOH electrodes extracted from CV and GCD.

No.	Materials	C_s from CV	C_s from GCD
1	Electropolymerized PEDOTOH:ClO ₄ in DCM with potentiostatic mode	197 F/g @ 10 mV/s	204.7 F/g @ 2.5 A/g
2	Electropolymerized PEDOTOH:ClO ₄ in water with potentiostatic mode	124.9 F/g @ 10 mV/s	94.9 F/g @ 6.15 A/g
3	Electropolymerized PEDOT:ClO ₄ in DCM with potentiostatic mode	100 F/g @ 10 mV/s	159.1 F/g @ 2.3 A/g
4	Electropolymerized PEDOTOH:ClO ₄ in DCM with galvanostatic mode	148 F/g @ 10 mV/s	120.7 F/g @ 3.9 A/g

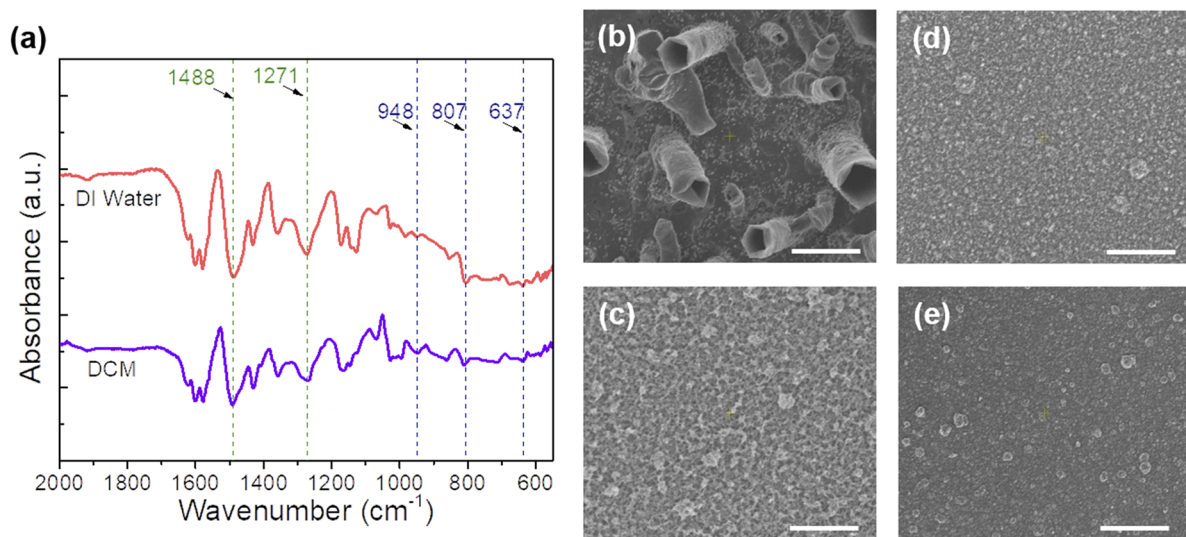


FIG. 3. Physicochemical characterizations of the PEDOTOH films. (a) FTIR spectra of PEDOTOH:ClO₄ in the range of 550 to 2000 cm⁻¹ showing the attributed peaks related with PEDOT polymerization. Top-view SEM images of PEDOTOH:ClO₄ fabricated in (b) DCM with potentiostatic mode, (c) DI water with potentiostatic mode, and (d) DCM with galvanostatic mode, while (e) PEDOT:ClO₄ produced in DCM with potentiostatic mode. Scale bar is 10 μm.

leading to poor capacitance retention and delamination. We evaluated the electrochemical stability of the polymer electrodes subjected to (i) 1000 CV cycles in the range -0.2 to 0.7 V at a scan rate of 50 mV s^{-1} and (ii) 1000 GCD cycles at a high current density of 5 mA cm^{-2} in 1 M LiClO_4 . Figure S6 displays selected CV cycles (i.e., first, 100th, 200th, 400th, 600th, 800th, and 1000th), and Fig. 4(a) displays the capacitance retention measured at the end of cycles for all the electrodes. We found that PEDOTOH:ClO₄ fabricated in DCM using potentiostatic or galvanostatic modes demonstrated capacitance retention of $\sim 84\%$ after

1000 CV cycles, whereas PEDOTOH:ClO₄ formed in DI water reached 76%. It should be noted that the polymer electrodes formed in DCM remained firmly intact on the substrate upon CV cycling and rinsing after the operation; in contrast, the polymer electrodes fabricated in DI water disintegrated into small fragments during the rinsing after CV cycling. While the PEDOT:ClO₄ fabricated in DCM exhibited the highest capacitance retention of 92% after 1000 CV cycles.

We further investigated the capacitance retention of each electrode from GCD plots since the latter electrochemical technique

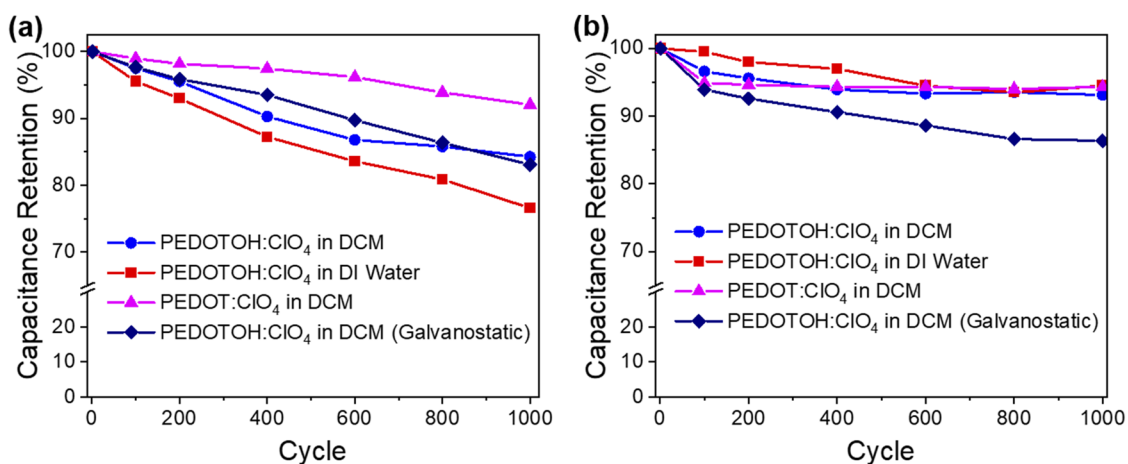


FIG. 4. Electrochemical stability and capacitance retention of PEDOTOH-based electrodes evaluated using (a) 1000 CV cycles and (b) 1000 charge–discharge cycles. The CV curves were recorded at a scan rate of 50 mV s^{-1} in 1 M LiClO_4 , while GCD curves were acquired at a current density of 5 mA cm^{-2} in 1 M LiClO_4 .

can replicate the supercapacitor profiles based on the current-driven operation. Interestingly, the electrodes showed good capacitance retention, lingering between 86% and 94% after 1000 GCD cycles at 5 mA cm^{-2} [Figs. 4(b) and S7]. We attribute this cycling stability to the porous networks manifested either as microtubes or as microfibers that mitigate the effect of repeated swelling/shrinking during ion movements in-and-out of the polymer bulk. The devised electrodes exhibited 100% Coulombic efficiency over the 1000 GCD cycles, highlighting the reversible (pseudo)-capacitive processes. Besides, the use of DCM as a medium for electropolymerization induces better adhesion between the deposited polymer and the underneath substrates without the need for customized EDOT derivatives or additional intermediate layers as proposed in the literature.^{26,43} Organic solvents, such as DCM, have low surface energy, enabling the polymer to better penetrate into the gold surface structure. In addition, since DCM can evaporate completely and faster than water, the electrodeposited polymer films can form better mechanical interlocking with the gold surface.⁴⁴ Therefore, based on the above-mentioned results on the specific capacitance, electrochemical stability, and adherence to the substrate, we selected

PEDOTOH:ClO₄ fabricated in DCM using the potentiostatic mode as the best performing polymer electrode for further investigation toward the potential applicability into supercapacitor devices.

Application in free-standing symmetrical supercapacitor devices

We fabricated a symmetrical supercapacitor device with two identical PEDOTOH microstructure electrodes in an agarose gel containing 1 M LiClO₄. Recently, gel-based electrolytes have attracted significant attention for energy storage devices due to easy handling, no leakage, moderate ionic conductivity, and flexibility for miniaturization and integration. Nikiforidis *et al.* have made self-standing supercapacitors by optimizing agarose gel electrolytes.³⁰ The resulting electrolytic system offered high energy and power density, operational flexibility, and fast response time by facilitating good ionic conductivity. Thus, we utilize a similar electrolytic platform system with optimized PEDOTOH microstructure electrodes for better performance. Figure 5(a) presents the rectangular CV profiles (the fill factor at 100 mV s^{-1} is equal to 86%) of the

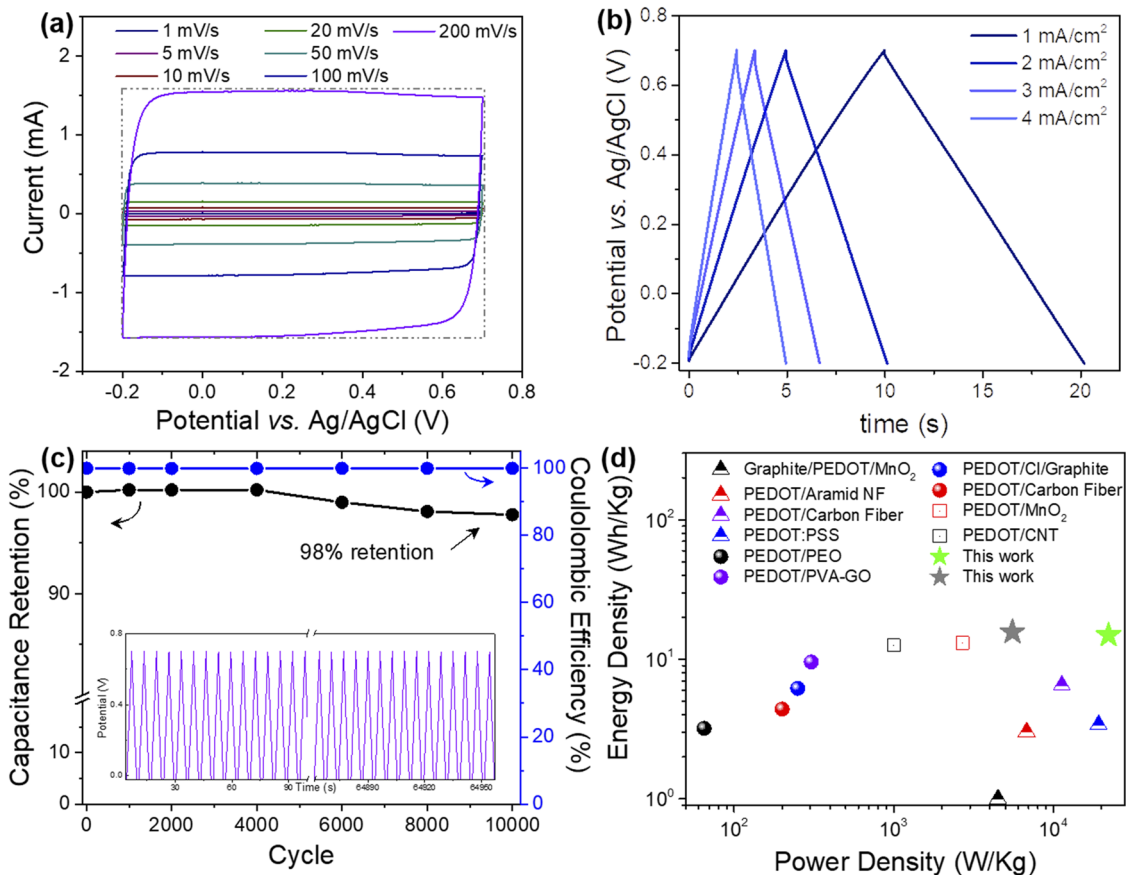


FIG. 5. Assembled PEDOTOH-based supercapacitor in an agarose gel electrolyte. (a) CV curves at different scan rates. (b) charge–discharge curves at different charging rates. (c) cycling stability, measured as capacitance retention after repeated cycling at 10 A g^{-1} . The corresponding Coulombic efficiency displays nearly 100% over 10000 cycles. (d) Comparative Ragone plots of the supercapacitors compared to other PEDOT-based supercapacitors.

supercapacitors, denoting exemplary capacitive behavior at different scan rates [Fig. S8(a)]. The GCD profiles at different current densities [1–4 mA cm⁻², Fig. 5(b)] verified the robust capacitive behavior of the supercapacitors, stemming from the perfect triangle shapes and indicating reversible pseudo(capacitive) processes at the polymer electrodes. The specific capacitances calculated from the discharge time with different current densities are plotted in Fig. S8(b). This supercapacitor achieves a specific capacitance of 38.8 F g⁻¹ at 3.6 A g⁻¹ and retains it at a threefold higher current density (i.e., 10 A g⁻¹ → 37 F g⁻¹). This high-rate capability validates the highly conductive and capacitive nature of the PEDOTOH microtube films, which, in turn, favor ion and electron transport at high rates.

Furthermore, on the basis of GCD data at a high current density of 10 A g⁻¹, the PEDOTOH electrodes retain 98% of their initial capacitance and exhibit a nearly 100% Coulombic efficiency after 10000 continuous cycles. Such electrochemical stability surpasses other conducting polymer-based supercapacitors, particularly those made of PEDOT electrodes (Table S3). Such outstanding cycling stability is attributed to the adherence of the PEDOTOH polymer to the substrate and the good structural stability of the material morphology that provides optimal networks for ion diffusion. This finding can also be expanded to explore the effect of the substrate morphology and other conducting substrates (e.g., nickel foam, carbon cloth, and ITO) for further improving the electrochemical properties and stability. Figure S9 depicts the Bode plots from EIS measurements before and after the GCD cycles. The impedance value and phase angle almost overlap at all frequencies, indicating negligible changes in the capacitance and resistance of the supercapacitors during long-term cycling. The τ_0 value is ~0.45 s, significantly shorter than other supercapacitors using aqueous-based electrolytes. The SEM images (Fig. S10) obtained before and after the GCD cycles display identical topology of the polymers, indicating a robust structural conformation of the polymer electrode during electrochemical operation. The supercapacitor made of PEDOTOH microtube electrodes achieves an energy density of 14.9 Wh kg⁻¹ at a power density of 22.2 kW kg⁻¹. This performance is better than several PEDOT-based supercapacitors recently reported in the literature, as illustrated in the Ragone plot of Fig. 5(d).

CONCLUSION

In summary, we have successfully fabricated PEDOTOH films with porous microstructures on the flexible Au/Kapton substrates that can be used as flexible electrodes for self-standing supercapacitors. The PEDOTOH porous microstructure was obtained by simply using a non-flammable solvent of DCM instead of the aqueous solution. The porous microstructure could increase the electrochemical active surface, facilitating the electrolyte penetration and resulting in higher specific capacitance. The optimal PEDOTOH electrodes generate a remarkable specific capacitance of 197.3 F g⁻¹ at a scan rate of 10 mV s⁻¹ or 204.7 F g⁻¹ at a charging rate of 1 mA cm⁻² (analogous to 2.5 A g⁻¹), which is 97.5% of the theoretical capacity of PEDOT (210 F g⁻¹). Furthermore, the assembled supercapacitors can lead to high capacitance (73.7 F g⁻¹ at a scan rate of 10 mV s⁻¹), good rate capability (37.1 F g⁻¹ at 10 A g⁻¹), and superior cyclability (98% capacitance retention over 10000 GCD cycles at 10 A g⁻¹). This symmetrical PEDOTOH-based supercapacitor

exhibited satisfactory performance, delivering an energy density of 14.9 Wh kg⁻¹ at a power density of 22.2 kW kg⁻¹ on par with other solely polymer-based supercapacitors. This work paves a simple and single-step fabrication recipe to improve the performance of pristine PEDOT-based electrodes for high-performance supercapacitors.

SUPPLEMENTARY MATERIAL

See the [supplementary material](#) for the complete electrochemical characterizations of the PEDOTOH electrodes.

ACKNOWLEDGMENTS

S.W. acknowledges a research grant program supported by Institut Teknologi Bandung (ITB) under Contract No. 0681/IT1.B05/KP/2021.

AUTHOR DECLARATIONS

Conflict of Interest

The authors have no conflicts to disclose.

DATA AVAILABILITY

The data that support the findings of this study are available from the corresponding authors upon reasonable request.

REFERENCES

- 1 P. Naskar, P. Chakraborty, D. Kundu, A. Maiti, B. Biswas, and A. Banerjee, "Envisaging future energy storage materials for supercapacitors: An ensemble of preliminary attempts," *ChemistrySelect* **6**(5), 1127 (2021).
- 2 J. Libich, J. Máca, J. Vondrák, O. Čech, and M. Sedlaříková, "Supercapacitors: Properties and applications," *J. Energy Storage* **17**, 224 (2018).
- 3 Y. Wang, Y. Song, and Y. Xia, "Electrochemical capacitors: Mechanism, materials, systems, characterization and applications," *Chem. Soc. Rev.* **45**(21), 5925 (2016).
- 4 G. Nikiforidis, M. E. Yagoubi, and M. Anouti, "Polarizable cesium cations for energy storage from electrolyte characterization to-EDLC application," *Electrochim. Acta* **402**, 139529 (2022).
- 5 N. R. Chodankar, H. D. Pham, A. K. Nanjundan, J. F. S. Fernando, K. Jayaramulu, D. Golberg, Y. K. Han, and D. P. Dubal, "True meaning of pseudocapacitors and their performance metrics: Asymmetric versus hybrid supercapacitors," *Small* **16**(37), 2002806 (2020).
- 6 S. G. Krishnan, A. Arulraj, M. Khalid, M. V. Reddy, and R. Jose, "Energy storage in metal cobaltite electrodes: Opportunities and challenges in magnesium cobalt oxide," *Renewable Sustainable Energy Rev.* **141**, 110798 (2021).
- 7 M. A. A. Mohd Abdah, N. H. N. Azman, S. Kulandaivalu, and Y. Sulaiman, "Review of the use of transition-metal-oxide and conducting polymer-based fibres for high-performance supercapacitors," *Mater. Des.* **186**, 108199 (2020).
- 8 Q. Meng, K. Cai, Y. Chen, and L. Chen, "Research progress on conducting polymer based supercapacitor electrode materials," *Nano Energy* **36**, 268 (2017).
- 9 G. A. Snook, P. Kao, and A. S. Best, "Conducting-polymer-based supercapacitor devices and electrodes," *J. Power Sources* **196**(1), 1 (2011).
- 10 I. Shown, A. Ganguly, L. C. Chen, and K. H. Chen, "Conducting polymer-based flexible supercapacitor," *Energy Sci. Eng.* **3**(1), 2 (2015).
- 11 M. J. Donahue, A. Sanchez-Sanchez, S. Inal, J. Qu, R. M. Owens, D. Mecerreyes, G. G. Malliaras, and D. C. Martin, "Tailoring PEDOT properties for applications in bioelectronics," *Mater. Sci. Eng.* **140**, 100546 (2020).

- ¹²A. Vadivel Murugan, M. V. Reddy, G. Campet, and K. Vijayamohan, "Cyclic voltammetry, electrochemical impedance and *ex situ* X-ray diffraction studies of electrochemical insertion and desinsertion of lithium ion into nanostructured organic-inorganic poly(3,4-ethylenedioxythiophene) based hybrids," *J. Electroanal. Chem.* **603**(2), 287 (2007).
- ¹³S. Panigrahy and B. Kandasubramanian, "Polymeric thermoelectric PEDOT: PSS & composites: Synthesis, progress, and applications," *Eur. Polym. J.* **132**, 109726 (2020).
- ¹⁴Z. Zhao, G. F. Richardson, Q. Meng, S. Zhu, H.-C. Kuan, and J. Ma, "PEDOT-based composites as electrode materials for supercapacitors," *Nanotechnology* **27**(4), 042001 (2015).
- ¹⁵P. Tang, L. Han, and L. Zhang, "Facile synthesis of graphite/PEDOT/MnO₂ composites on commercial supercapacitor separator membranes as flexible and high-performance supercapacitor electrodes," *ACS Appl. Mater. Interfaces* **6**(13), 10506 (2014).
- ¹⁶S. Ahmed and M. Rafat, "Hydrothermal synthesis of PEDOT/rGO composite for supercapacitor applications," *Mater. Res. Express* **5**(1), 015507 (2018).
- ¹⁷X. He, W. Yang, X. Mao, L. Xu, Y. Zhou, Y. Chen, Y. Zhao, Y. Yang, and J. Xu, "All-solid state symmetric supercapacitors based on compressible and flexible free-standing 3D carbon nanotubes (CNTs)/poly(3,4-ethylenedioxythiophene) (PEDOT) sponge electrodes," *J. Power Sources* **376**, 138 (2018).
- ¹⁸Z. Yu, L. Tetard, L. Zhai, and J. Thomas, "Supercapacitor electrode materials: Nanostructures from 0 to 3 dimensions," *Energy Environ. Sci.* **8**(3), 702 (2015).
- ¹⁹J. M. D'Arcy, M. F. El-Kady, P. P. Khine, L. Zhang, S. H. Lee, N. R. Davis, D. S. Liu, M. T. Yeung, S. Y. Kim, C. L. Turner *et al.*, "Vapor-phase polymerization of nanofibrillar poly(3,4-ethylenedioxythiophene) for supercapacitors," *ACS Nano* **8**(2), 1500 (2014).
- ²⁰Y. Koshiba, M. Hirai, S. Horike, T. Fukushima, and K. Ishida, "Preparation of poly(3,4-ethylenedioxythiophene) by vapor-phase polymerization at the interface between 3,4-ethylenedioxythiophene vapor and oxidant melt," *Mol. Cryst. Liq. Cryst.* **688**(1), 53 (2019).
- ²¹J. Rehmen, K. Zuber, M. Modarresi, D. Kim, E. Charrault, P. Jannasch, I. Zozoulenko, D. Evans, and C. Karlsson, "Structural control of charge storage capacity to achieve 100% doping in vapor phase-polymerized PEDOT/Tosylate," *ACS Omega* **4**(26), 21818 (2019).
- ²²X. Chen, F. Jiang, Q. Jiang, Y. Jia, C. Liu, G. Liu, J. Xu, X. Duan, C. Zhu, G. Nie *et al.*, "Conductive and flexible PEDOT-decorated paper as high performance electrode fabricated by vapor phase polymerization for supercapacitor," *Colloids Surf., A* **603**, 125173 (2020).
- ²³X. Cui and D. C. Martin, "Electrochemical deposition and characterization of poly(3,4-ethylenedioxythiophene) on neural microelectrode arrays," *Sens. Actuators, B* **89**(1), 92 (2003).
- ²⁴G. Nikiforidis, S. Wustoni, C. Routier, A. Hama, A. Koklu, A. Saleh, N. Steiner, V. Druet, H. Fiumelli, and S. Inal, "Benchmarking the performance of electropolymerized poly(3,4-ethylenedioxythiophene) electrodes for neural interfacing," *Macromol. Biosci.* **20**(11), 2000215 (2020).
- ²⁵B. Wei, J. Liu, L. Ouyang, C.-C. Kuo, and D. C. Martin, "Significant enhancement of PEDOT thin film adhesion to inorganic solid substrates with EDOT-acid," *ACS Appl. Mater. Interfaces* **7**(28), 15388 (2015).
- ²⁶L. Ouyang, B. Wei, C. C. Kuo, S. Pathak, B. Farrell, and D. C. Martin, "Enhanced PEDOT adhesion on solid substrates with electrografted P(EDOT-NH₂)," *Sci. Adv.* **3**(3), e1600448 (2017).
- ²⁷Y.-K. Hsu, Y.-C. Chen, Y.-G. Lin, L.-C. Chen, and K.-H. Chen, "Direct-growth of poly(3,4-ethylenedioxythiophene) nanowires/carbon cloth as hierarchical supercapacitor electrode in neutral aqueous solution," *J. Power Sources* **242**, 718 (2013).
- ²⁸G. P. Pandey, A. C. Rastogi, and C. R. Westgate, "All-solid-state supercapacitors with poly(3,4-ethylenedioxythiophene)-coated carbon fiber paper electrodes and ionic liquid gel polymer electrolyte," *J. Power Sources* **245**, 857 (2014).
- ²⁹B. Anothumakkool, A. Torris A. T., S. N. Bhang, M. V. Badiger, and S. Kurungot, "Electrodeposited polyethylenedioxythiophene with infiltrated gel electrolyte interface: A close contest of an all-solid-state supercapacitor with its liquid-state counterpart," *Nanoscale* **6**(11), 5944 (2014).
- ³⁰G. Nikiforidis, S. Wustoni, D. Ohayon, V. Druet, and S. Inal, "A self-standing organic supercapacitor to power bioelectronic devices," *ACS Appl. Energy Mater.* **3**(8), 7896 (2020).
- ³¹S. Wustoni, T. C. Hidalgo, A. Hama, D. Ohayon, A. Savva, N. Wei, N. Wehbe, and S. Inal, "In situ electrochemical synthesis of a conducting polymer composite for multimetabolite sensing," *Adv. Mater. Technol.* **5**(3), 1900943 (2020).
- ³²S. Zhang, J. Xu, B. Lu, L. Qin, L. Zhang, S. Zhen, and D. Mo, "Electrochromic enhancement of poly(3,4-ethylenedioxythiophene) films functionalized with hydroxymethyl and ethylene oxide," *J. Polym. Sci., Part A: Polym. Chem.* **52**(14), 1989 (2014).
- ³³S. Akoudad and J. Roncali, "Modification of the electrochemical and electronic properties of electrogenerated poly(3,4-ethylenedioxythiophene) by hydroxymethyl and oligo(oxyethylene) substituents," *Electrochem. Commun.* **2**(1), 72 (2000).
- ³⁴M. C. Simoes, K. J. Hughes, D. B. Ingham, L. Ma, and M. Pourkashanian, "Estimation of the thermochemical radii and ionic volumes of complex ions," *Inorg. Chem.* **56**(13), 7566 (2017).
- ³⁵Y. Lu, Y.-p. Wen, B.-y. Lu, X.-m. Duan, J.-k. Xu, L. Zhang, and Y. Huang, "Electrosynthesis and characterization of poly(hydroxy-methylated-3,4-ethylenedioxythiophene) film in aqueous micellar solution and its biosensing application," *Chin. J. Polym. Sci.* **30**(6), 824 (2012).
- ³⁶Y. Xiao, X. Cui, J. M. Hancock, M. Bouguettaya, J. R. Reynolds, and D. C. Martin, "Electrochemical polymerization of poly(hydroxymethylated-3,4-ethylenedioxythiophene) (PEDOT-MeOH) on multichannel neural probes," *Sens. Actuators, B* **99**(2), 437 (2004).
- ³⁷C. Pitsalidis, A. M. Pappa, M. Porel, C. M. Artim, G. C. Faria, D. D. Duong, C. A. Alabi, S. Daniel, A. Salleo, and R. M. Owens, "Biomimetic electronic devices for measuring bacterial membrane disruption," *Adv. Mater.* **30**(39), 1803130 (2018).
- ³⁸S. Wustoni, C. Combe, D. Ohayon, M. H. Akhtar, I. McCulloch, and S. Inal, "Membrane-free detection of metal cations with an organic electrochemical transistor," *Adv. Funct. Mater.* **29**(44), 1904403 (2019).
- ³⁹B. Li, H. Lopez-Beltran, C. Siu, K. H. Skorenko, H. Zhou, W. E. Bernier, M. S. Whittingham, and W. E. Jones, "Vapor phase polymerized PEDOT/cellulose paper composite for flexible solid-state supercapacitor," *ACS Appl. Energy Mater.* **3**(2), 1559 (2020).
- ⁴⁰Y. Yang, L. Zhang, S. Li, W. Yang, J. Xu, Y. Jiang, and J. Wen, "Electrochemical performance of conducting polymer and its nanocomposites prepared by chemical vapor phase polymerization method," *J. Mater. Sci.: Mater. Electron.* **24**(7), 2245 (2013).
- ⁴¹Q. Zhao, R. Jamal, L. Zhang, M. Wang, and T. Abdiryim, "The structure and properties of PEDOT synthesized by template-free solution method," *Nanoscale Res. Lett.* **9**(1), 557 (2014).
- ⁴²C. T. Ly, C. T. Phan, C. N. Vu, H. S. Le, T. T. Nguyen, D. L. Tran, L. A. Le, and T. T. Vu, "Electrodeposition of PEDOT-rGO film in aqueous solution for detection of acetaminophen in traditional medicaments," *Adv. Nat. Sci.: Nanosci. Nanotechnol.* **10**(1), 015013 (2019).
- ⁴³E. Villemin, B. Lemarque, T. T. Vü, V. Q. Nguyen, G. Trippé-Allard, P. Martin, P.-C. Lacaze, and J.-C. Lacroix, "Improved adhesion of poly(3,4-ethylenedioxythiophene) (PEDOT) thin film to solid substrates using electrografted promoters and application to efficient nanoplasmonic devices," *Synth. Met.* **248**, 45 (2019).
- ⁴⁴G. Jun, J.-W. Lee, Y. Shin, K. Kim, and W. Hwang, "Solvent-aided direct adhesion of a metal/polymer joint using micro/nano hierarchical structures," *J. Mater. Process. Technol.* **285**, 116744 (2020).